Chinese Chemical Letters 37 (2026) 111407

Contents lists available at ScienceDirect

Chinese Chemical Letters

journal homepage: www.elsevier.com/locate/cclet

Monofluoroiodane(III) reagent mediated Wagner–Meerwein rearrangement fluorination: Construction of quaternary C(sp^3)–F bond

Jing Ren[a,b,1,*], Feng-Huan Du[a,1], Xiaowei Chen[a], Chi Zhang[a,*]

[a] State Key Laboratory of Elemento-Organic Chemistry, The Research Institute of Elemento-Organic Chemistry, College of Chemistry, Nankai University, Tianjin 300071, China
[b] Shanxi Bethune Hospital, Shanxi Academy of Medical Sciences, Tongji Shanxi Hospital, Third Hospital of Shanxi Medical University, Taiyuan 030032, China

ARTICLE INFO

Article history:
Received 4 March 2025
Revised 22 May 2025
Accepted 3 June 2025
Available online 4 June 2025

Keywords:
Monofluoroiodane(III) reagent
Silver(I)-catalysis
Wagner-Meerwein rearrangement
Fluorination
DFT

ABSTRACT

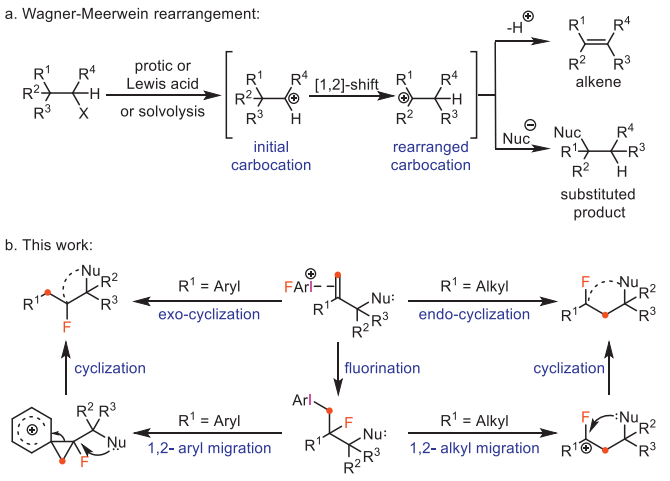
Fluoroorganic chemistry is one of the most hectic areas of current chemical research, exerting a profound effect on the most vital industries such as medicine, pesticide, and material science. Synthesis of fluorine-containing organic molecules, particularly those that bear C(sp^3)–F bonds, remains a great challenge in modern chemical synthesis. Herein, we disclose a new strategy for the construction of a carbon–fluorine quaternary center, which was accomplished with the silver(I)-catalyzed intramolecular Wagner–Meerwein rearrangement fluorination of allylic gem-disubstituted alkene derivatives by using a hypervalent monofluoroiodine(III) reagent **1** (**AFBI**). Interestingly, the tunable five/six-membered heterocycle selectivity is achieved by the intramolecular Wagner–Meerwein rearrangement fluorination *via* a judicious choice of the group R^1 attached to the C–C double bond. This versatile strategy features simple starting materials, mild reaction conditions, good functional-group compatibility, high bond-forming efficiency (*e.g.*, one C–F and one C–O bond), and excellent chemoselectivity. The proposed reaction mechanisms and the roles of the catalyst $AgBF_4$ were understood by control experiments and density functional theory calculations.

© 2026 Published by Elsevier B.V. on behalf of Chinese Chemical Society and Institute of Materia Medica, Chinese Academy of Medical Sciences.

Wagner–Meerwein reaction, as a classical carbocation rearrangement reaction, is of great significance in organic synthesis and biosynthetic chemistry [1]. The contemporary description of Wagner–Meerwein rearrangements includes 1,2-cationic migrations of alkyl and aryl groups as well as hydride (Scheme 1a) [2]. It is widely known that hypervalent iodine reagents, as a class of non-metallic oxidants, owing to their electrophilic nature and excellent leaving-group ability, have been widely used in various types of organo-oxidative rearrangement reactions [3–7]. These particular oxidative rearrangement reactions include [1,2]-migration [8–12], Hofmann rearrangement [13–15], Beckmann rearrangement [16,17], Curtius rearrangement [18], ring contraction [19–23]/expansion [24–26], and [3,3]-sigmatropic/iodonium–Claisen rearrangement [27,28]. Although some elegant Wagner–Meerwein reactions induced by hypervalent fluoroiodane(III) reagents have been reported [29–35], these reactions can only lead to [1,2]-aryl migrated fluorinated products. Wagner–Meerwein rearrangement fluorination of [1,2]-alkyl or aryl group migration simultaneously mediated by hypervalent fluoroiodane(III) reagent has rarely been reported to date, which we attribute to the formidable challenge involved in controlling the selective rearrangement of the highly active carbocation intermediates [36,37]. Recently, the elegant study represented by asymmetric 1,3-difluorinative Wagner–Meerwein rearrangement of β-substituted styrene derivatives [38] has been developed, and two different mechanisms are operative. Lately, Zhang group reported a novel hypervalent fluoroiodane(III) reagent **1**, which is an air- and moisture-stable compound and has been successfully used for metal-free carbon–carbon bond scission and intramolecular ring expansion fluorination of unactivated cyclopropanes [26]. Another appealing advantage is that reagent **1** could be prepared simply by oxy-fluorination of corresponding aryl iodides with commercially available silver difluoride, avoiding the use of multi-step ligand exchange reactions [39]. We wondered whether Wagner–Meerwein rearrangement fluorination could be achieved by reagent **1**. We hypothesized that if nucleophilic substituents were present on the *gem*-disubstituted alkenes derivatives, Wagner–Meerwein rearrangement fluorination of [1,2]-alkyl or aryl group migration and intramolecular cyclization might be achieved, and the reaction might form quaternary carbon centers containing C(sp^3)–F bond with excellent chemo-selectivity (Scheme 1b). The construction of

* Corresponding authors.
E-mail addresses: renjing1114@126.com (J. Ren), zhangchi@nankai.edu.cn (C. Zhang).
[1] These authors contributed equally to this work.

https://doi.org/10.1016/j.cclet.2025.111407
1001-8417/© 2026 Published by Elsevier B.V. on behalf of Chinese Chemical Society and Institute of Materia Medica, Chinese Academy of Medical Sciences.

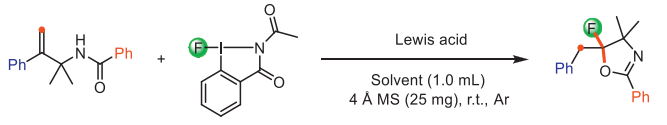


Scheme 1. (a) Wagner–Meerwein rearrangement. (b) Monofluoroiodane(III) reagent mediated Wagner–Meerwein rearrangement (this work).

C(sp^3)–F bond is an important yet challenging task in organic synthesis. Recently, Feng's group reported sulfone as a traceless activating group for constructing the C–F quaternary stereocenter [40]. It is worth noting that many marketed best-selling drugs featuring C(sp^3)–F quaternary carbon centers, such as fludrocortisone [41], fluticasone propionate [42], and sofosbuvir [43].

In the initial reactions, we employed allylic *gem*-disubstituted alkenes with tethered amide groups as substrates in the presence of fluoroiodane(III) reagent **1** as fluorine source in anhydrous dichloromethane (Table 1). We selected *N*-(2-methyl-3-phenylbut-3-en-2-yl)benzamide **2a** as a model substrate for the optimization of the reaction conditions. The reaction of **2a** and **1** (1.5 equiv.) afforded 5-benzyl-5-fluoro-4,4-dimethyl-2-phenyl-4,5-dihydrooxazole (**3a**, 27 % yield) in the presence of 4 Å molecular sieve (25 mg) in anhydrous dichloromethane at room temperature for 12 h (Table 1, entry 1). Encouraged by this result, we carried out experiments to improve the chemical yield of **3a**. The reaction yield was increased to 74 % when $AgBF_4$ (1.0 equiv.) was used (Table 1, entry 2). Next, we studied the solvent effect on the reaction. With the use of $AgBF_4$ (1.0 equiv.), anhydrous dichloromethane was replaced by anhydrous acetonitrile, affording **3a** with a low yield of 58 % (Table 1, entry 3). The lower yield was obtained by using HBF_4 (1.0 equiv.) instead of $AgBF_4$ (1.0 equiv.) (Table 1, entry 4). To our delight, decreasing the amount of $AgBF_4$ from 1.0 to 0.1 equiv. increased the yield of **3a** to 79 % (Table 1, entry 5). In addition, $AgBF_4$ proved to be the best catalyst, as $Zn(BF_4)_2$ and $BF_3{\cdot}OEt_2$ gave the amounts of **3a** in 65 % and 50 % yield, respectively (Table 1, entries 6 and 7). When 1.2 equiv. reagent **1** were used, the yield of **3a** was reduced to 61 % yield (Table 1, entry 8). The yields slightly decreased when the reaction was performed under the air atmosphere (Table 1, entry 9).

Table 1
Optimization of reaction conditions[a].



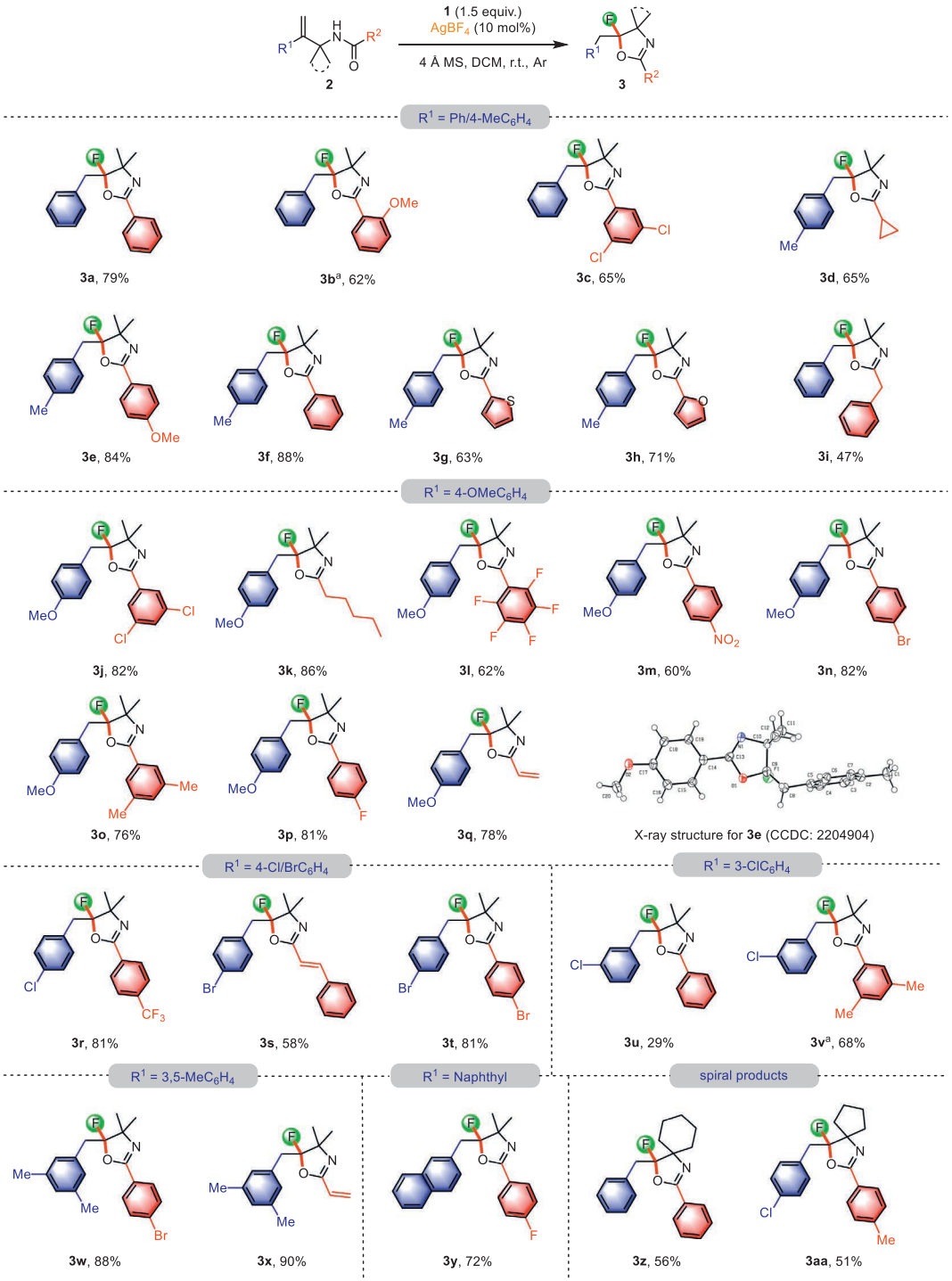
2a fluoroiodane **1** 3a

Entry	Solvent	**1** (equiv.)	Lewis acid (equiv.)	Time (h)	**3a** yield (%)[b]
1	DCM	1.5	-	12	27
2	DCM	1.5	$AgBF_4$ (1)	4	74
3	MeCN	1.5	$AgBF_4$ (1)	4	58
4	DCM	1.5	HBF_4 (1)	2.5	23
5	DCM	1.5	$AgBF_4$ (10 %)	4	79
6	DCM	1.5	$Zn(BF_4)_2$ (10 %)	4	65
7	DCM	1.5	$BF_3{\cdot}OEt_2$ (10 %)	4	50
8	DCM	1.2	$AgBF_4$ (10 %)	4	61
9[c]	DCM	1.5	$AgBF_4$ (10 %)	6	73

[a] Reaction conditions: allylic *gem*-disubstituted alkene **2a** (0.1 mmol, 1.0 equiv.), fluoroiodane **1** (1.2–1.5 equiv.), a Lewis acid, and 4 Å molecular sieves (25 mg) were stirred in 1 mL of solvent at room temperature.
[b] Yield after purification by column chromatography.
[c] Under air atmosphere.

With the optimized conditions in hand (Table 1, entry 5), we were next intrigued to explore the generality and functional group compatibility of the developed protocol. As shown in Scheme 2, the *ortho*-methoxy substituted **2b** could also undergo this transformation to deliver the desired products **3b**. The substrate **2c** containing 3,5-dichloro substituent also proceeded smoothly to give **3c** in 65 % yield. Subsequently, we maintained R^1 as 4-MeC_6H_4 and screened a variety of substrates. Pleasantly, when R^2 group was cyclopropyl (**2d**), 4-$OMeC_6H_4$ (**2e**), phenyl (**2f**), 2-thienyl (**2g**), or 2-furanyl (**2h**), the reaction exhibited high activities, delivering the corresponding products **3d**–**3h** in 63 %–88 % yields. When R^2 was benzyl, we obtained a 47 % yield of the desired product **3i** for 4 h at room temperature. Besides, the configuration of **3e** was unambiguously determined by the X-ray crystallographic analysis. Also, when R^1 was 4-$OMeC_6H_4$, the substrates bearing 3,5-ClC_6H_3 (**2j**), *n*-pentyl (**2k**), perfluorophenyl (**2l**), 4-$NO_2C_6H_4$ (**2m**), 4-BrC_6H_4 (**2n**), 3,5-MeC_6H_3 (**2o**), 4-FC_6H_4 (**2p**) as well as vinyl (**2q**) were all compatible with this protocol. Noteworthy, the present transformation worked well when there was an electron-withdrawing substituent (chlorine or bromine) in the *para*-position of the phenyl ring, and the desired products **3r**–**3t** were formed in the good to excellent yields. Specifically, when chlorine atom was present in the meta- position of the phenyl ring, the substrate **2u** reacted slowly at room temperature to form the target product **3u** in 29 % yield, with 30 % of the starting material recovered. Of note, for the substrate **2v**, the desired product **3v** was isolated in 68 % yield by increasing the reaction temperature to 40 °C. When R^1 was 3,5-MeC_6H_3, two substrates bearing 4-BrC_6H_4 (**2w**) as well as vinyl (**2x**) were all compatible in the present reaction, giving the desired products **3w** and **3x** in 88 % and 90 % yield, respectively. In the case where R^1 is a naphthyl group, the substrate **2y** also exhibited good reactivity, giving the product **3y** in 72 % yield. Moreover, the substrates containing a cycloalkyl framework were found to be suitable for this system, affording spiral products **3z** and **3aa** in good yields.

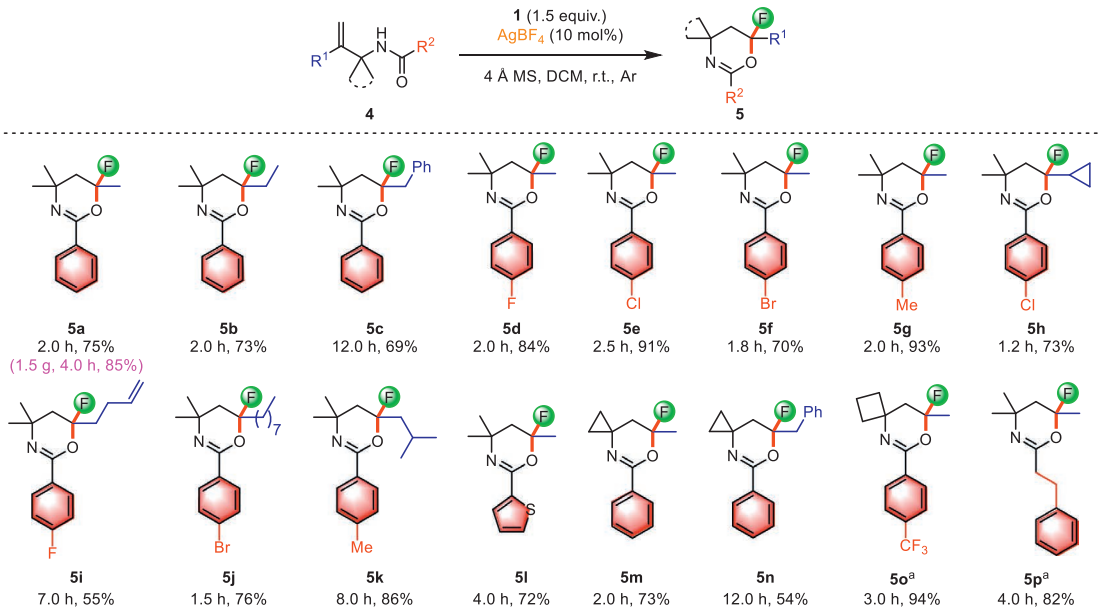
Next, we chose *N*-(2,3-dimethylbut-3-en-2-yl)benzamide **4a** as a substrate to explore its reaction with reagent **1**. To our surprise, reaction of **4a** and **1** (1.5 equiv.) afforded 6-fluoro-4,4,6-trimethyl-2-phenyl-5,6-dihydro-4*H*-1,3-oxazine (**5a**, 75 % yield) in the presence of $AgBF_4$ (0.1 equiv.) and 4 Å molecular sieves (37 mg). In this reaction, we did not detect the five-membered oxazole ring fluorinated product, but obtained the six-membered oxazine ring fluorinated one, showing the excellent chemoselectivity of the reaction. We speculated that the reaction may have followed a different migration pathway. This finding inspired us to expand the scope of the discovered reaction to synthesize other six-membered oxazine ring fluorinated compounds, and the experimental results are summarized in Scheme 3. Substrates **4b** and **4c** with diverse alkyl groups (Et and Bn) as R^1 group have also been proven to be suitable substrates, which participated in the reaction smoothly to produce products **5b** and **5c** in 73 % and 69 % yields, respectively. When R^1 in the substrate was methyl group (**4d**-**4g**), the reaction conditions provided reliable good yields; in most cases, the aromatic ring of R^2 with different para substituents had no significant effect on the product yields. Importantly, this rearrangement fluorination protocol was compatible with a variety of alkyl sub-



Scheme 2. Substrate scope for the 1,2-aryl migration. Reaction condition: allylic *gem*-disubstituted alkenes **2** (0.15 mmol, 1.0 equiv.), fluoroiodane **1** (0.225 mmol, 1.5 equiv.), $AgBF_4$ (0.015 mmol, 10 mol%), 4 Å molecular sieves (37 mg) were stirred in dry DCM (0.1 mol/L) at room temperature. Yield after purification by column chromatography. [a] Reaction was conducted at 40 °C.

stituents, including cyclopropyl (**4h**), 1-butylenyl (**4i**), *n*-heptyl (**4j**), and isobutyl with large steric hindrance (**4k**), the reaction exhibited high activities, delivering the corresponding products **5h**–**5k** in 55 %–86 % yields. When the substrate containing heteroaromatic substituent (**4l**) the reaction proceeded smoothly, delivering the corresponding product **5l** in a 72 % yield. Moreover, the substrates containing a cycloalkyl framework were found to be suitable for this system, affording spiral ring products **5m**–**5o** in 54 %–94 % yields. Furthermore, the structure of **5m** was identified by X-ray diffraction (Fig. 1). Also, when R^2 was ethylbenzene, the substrate **4p** was compatible with this protocol and the desired product **5p** was obtained in 82 % yield. To assess the scalability of the reaction, a gram-scale synthesis was conducted under standard conditions, affording product **5a** (1.5 g) in 85 % isolated yield.

To gain insight into the mechanism of fluoroiodane(III) reagent **1** mediated Wagner–Meerwein rearrangement fluorination, we conducted an array of control experiments (Scheme 4). To understand the difference in reaction rate between the above two reactions, we reacted **2a** and **4a** (the molar ratio of substrate **2a** to **4a** is 1:1) with fluoroiodane(III) reagent **1** under the standard re-



Scheme 3. Substrate scope for the 1,2-alkyl migration. Reaction condition: allylic *gem*-disubstituted alkenes **4** (0.15 mmol, 1.0 equiv.), fluoroiodane **1** (0.225 mmol, 1.5 equiv.), $AgBF_4$ (0.015 mmol, 10 mol %), 4 Å molecular sieves (37 mg) were stirred in dry DCM (0.1 mol/L). Yield after purification by column chromatography. [a] The products have a low boiling point and evaporation temperature under reduced pressure is less than 15 °C.

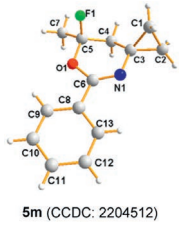
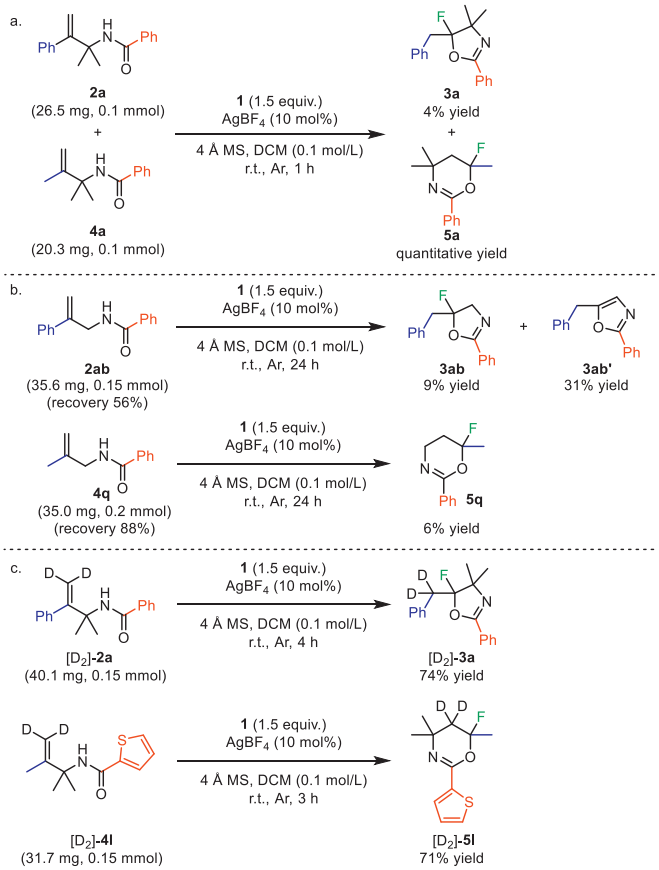


Fig. 1. ORTEP drawing of **5m** with thermal ellipsoids at 50 % probability.

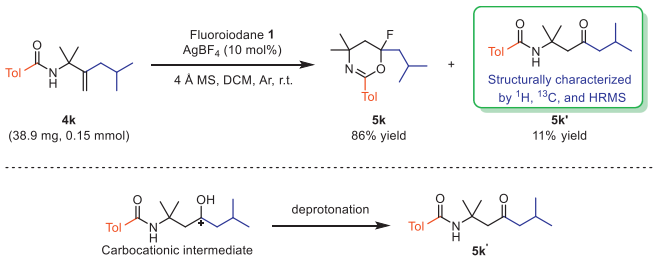
action conditions (Scheme 4a). This competitive reaction resulted in a yield of only 4 % for **3a**, compared to a quantitative yield for **5a**, thus indicating that the generation of **5a** is faster than that of **3a**, which provides a clue for the subsequent theoretical calculation investigation for the reaction mechanism. To demonstrate the importance of the dimethyl moiety of the substrates as an essential auxiliary for the success, substrate **2ab** without the dimethyl moiety was tested. The desired fluorinated product **3ab** was obtained in only 9 % yield and 56 % of the starting material **2ab** was recovered after 24 h, while the elimination by-product **3ab'** was formed in 31 % yield (Scheme 4b). Similarly, when **4q** was subjected to the standard reaction conditions, the desired fluorinated cyclized product was formed in only 6 % yield after 24 h, with 88 % of **4q** remaining unreacted. These results obtained demonstrate the indispensability of the dimethyl moiety for the success of the reaction (Scheme 4b). Next, a series of H/D exchange and deuterium-labelling experiments were performed to probe the manner of the disconnection and formation of chemical bonds during the reaction (Scheme 4c). When $[D_2]$-**2a** reacted with **1** in the presence of $AgBF_4$ under the standard reaction conditions, a 74 % yield of the compound $[D_2]$-**3a** was obtained in a very clean reaction. The analysis of product $[D_2]$-**3a** revealed that the isotopically labelled atoms are exclusively located in the benzylic position of **3a**, clearly demonstrating the 1,2-shift of the aryl group in substrate **2a**. Furthermore, when $[D_2]$-**4l** was treated with **1**, we obtained a 1,2-shift of the alkyl group deuterated product $[D_2]$-**5l** in a 71 % yield.

Interestingly, under standard reaction conditions, we successfully separated the by-product **5k'** by reacting the substrate **4k**



Scheme 4. (a) Study on the difference in reaction rate between the two reactions. (b) Study on the reactivity of the substrates exerted by the dimethyl substitution. (c) The experiments with isotopically labelled $[D_2]$-**2a** and $[D_2]$-**4l**.

with **1**. The formation of **5k'** could be due to a deprotonation reaction of a tertiary carbocation intermediate. Analysis of the by-product **5k'** revealed that trace water in the system competed with fluorine anion for nucleophilic reaction, then 1,2-alkyl migration occurred, and the deprotonation could afford **5k'** (Scheme 5). This



Scheme 5. Experiment to probe the mechanism for fluorination–migration–cyclization.

experiment illustrated that the present reaction might proceed *via* a fluorination–migration–cyclization process.

To further understand the mechanism of the above **AFBI** mediated cyclofluorination reaction of **2a**, we performed the density functional theory (DFT) calculations on the reaction of substrate **2a** and **AFBI**, as well as the reaction of **4a** and **AFBI**, and the corresponding calculated Gibbs free energy profiles are depicted in Figs. 2 and 3, respectively. Regarding to the reaction of **2a** and **AFBI**, the calculation result shows that the reaction is initiated by the formation of **IM1** from **AFBI** and catalyst $AgBF_4$ following a "F−coordination" activation mode [44,45] with the decrease of energy by 4.2 kcal/mol. To illustrate the enhancing effect of $AgBF_4$ on the reactivity of **AFBI**, we conducted the electronic structure calculations to compare the energy of the respective anti-bonding orbital of the 3c-4e hypervalent bonds of **AFBI** and **IM1**. The presence of $AgBF_4$ reduces the energy of the anti-bonding orbital of **AFBI** from -1.30 eV to -2.18 eV. This observation demonstrates that, with the aid of $AgBF_4$, **IM1** is capable of receiving electrons with greater ease than **AFBI** itself. Then, **IM1** undergoes an electrophilic addition to the olefinic double bond in the substrate **2a** to give the cyclic iodonium intermediate **IM2**. Subsequently, the fluoride anion attacks the most substituted carbon of the olefinic double bond to form **IM3**, which must overcome an activation energy barrier of 23.5 kcal/mol, making this the rate-determining step in the reaction. From **IM2** to **IM3**, Ag(I) stabilises the fluoride anion generated by the coordination of the olefinic double bond with the iodine(III) centre, thus promoting the formation of C-F bond. With the help of $AgBF_4$, the benziodazolone skeleton undergoes a conformational change due to the rotation of the N-Ac bond in **IM3**, leading to the formation of **IM4** with an energy barrier of 5.4 kcal/mol. In **IM4**, Ag(I) forms a stable 18-electrons complex with BF_4^- and two oxygen atoms on the benziodazolone skeleton. The phenyl migration occurs *via* a three-membered ring transition state **TS3**, which requires overcoming an activation energy barrier of 11.3 kcal/mol relative to **IM4**. In particular, the four-coordination mode for Ag(I) reduces the energy by 13.5 kcal/mol compared to that of the three-coordinated transition state **TS3-2**. In **TS3**, Ag(I) catalyst weakens the hypervalent iodine bond and enhances the leaving group ability of aryl iodine by coordinating with oxygen atoms of two carbonyl groups. This migration step results in the formation of the carbocation intermediate **IM5** and an Ag(I) complex **G-AgBF$_4$** with *N*-acetylbenziodazolone ligand. The competing [1,2]-aminoalkyl migration must overcome an energy barrier of 15.1 kcal/mol, which is much higher than that required for [1,2]-phenyl migration (11.3 kcal/mol), indicating that the [1,2]-phenyl migration is more favourable than [1,2]-aminoalkyl migration. Finally, **IM5** forms a more thermodynamically favourable cyclization product **3a**, which is exothermic by 64.7 kcal/mol. The effect of *gem*-dimethyl group can be explained by the Thorpe-Ingold effect, which suggests that the introduction of *gem*-dimethyl groups onto the carbon chains of substrates can facilitate the cyclization reactions by reducing the bond angles of the carbon chains. In **IM5**, the bond angle of C-C-N is 109°, whereas in the absence of the *gem*-dimethyl group, the angle of C-C-N is 115° in **IM5-1**, which

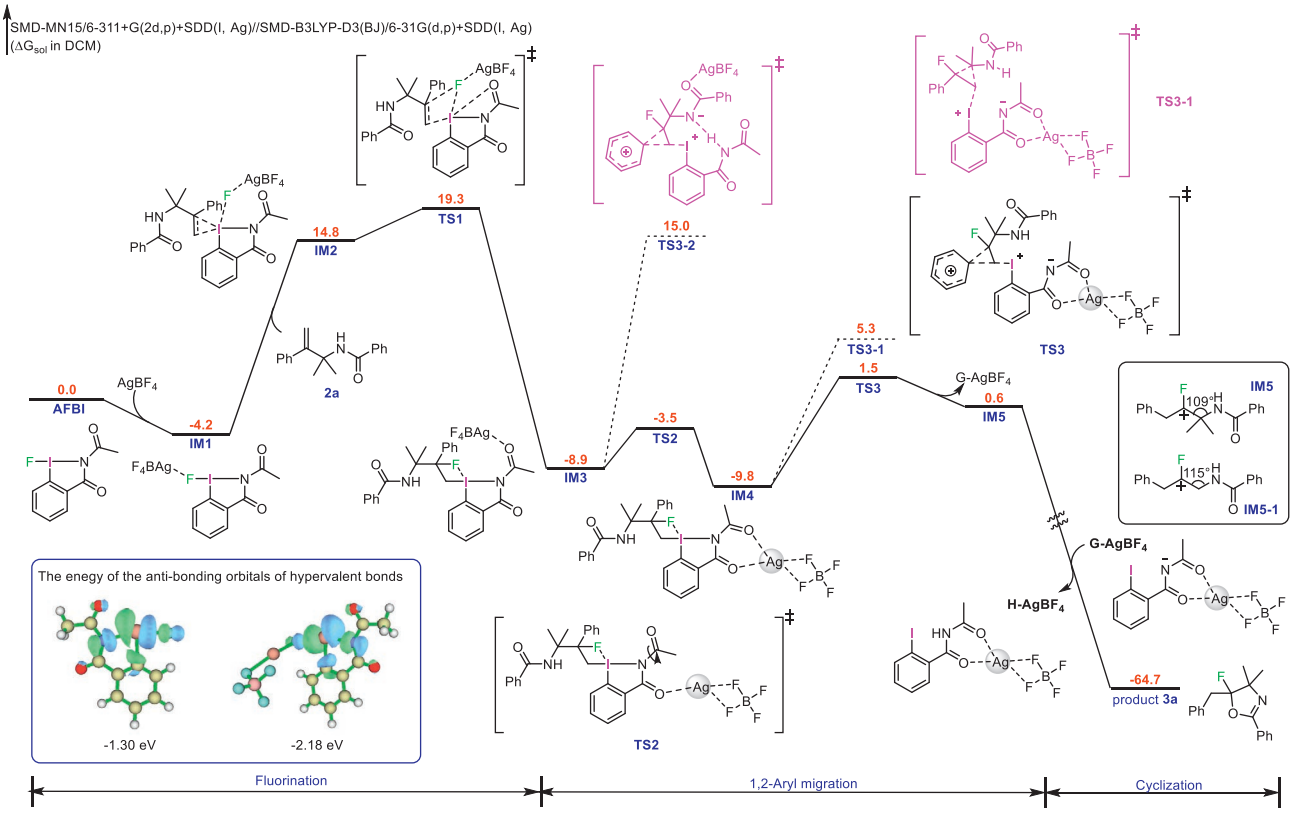


Fig. 2. DFT-computed potential energy profile for the reaction between **2a** and reagent **1** (standard state: 25 °C, 1 mol/L).

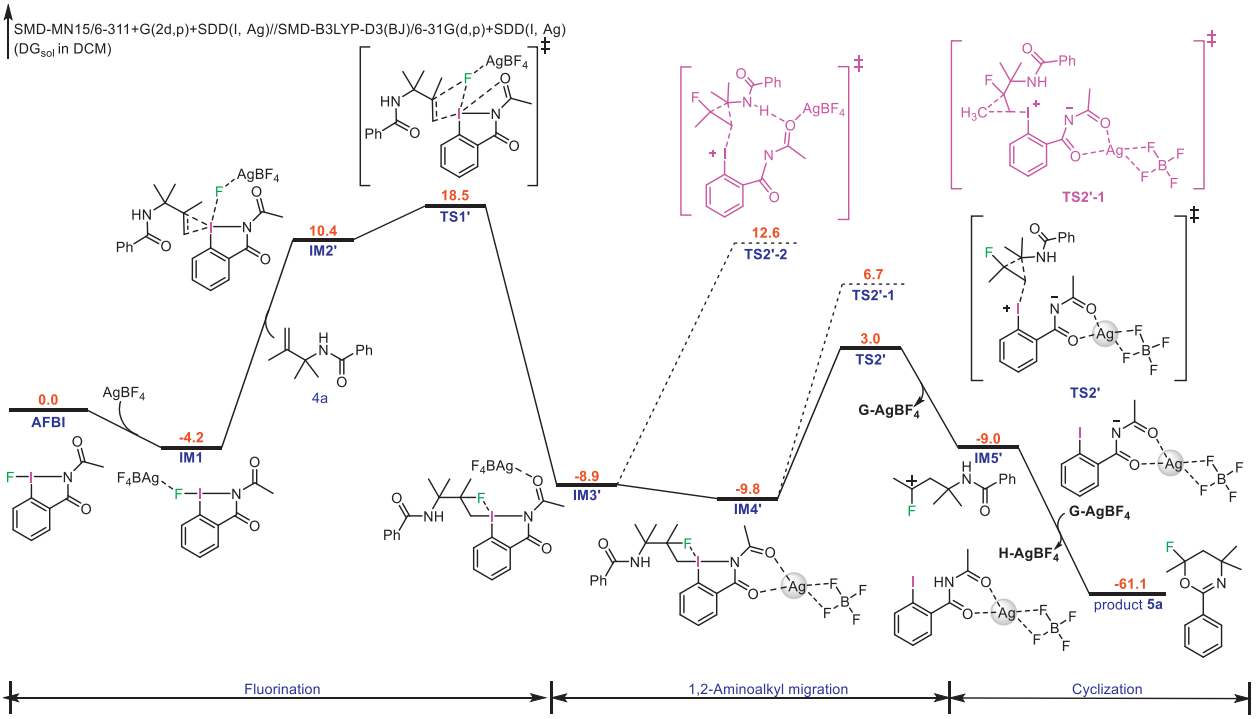


Fig. 3. DFT-computed potential energy profile for the reaction between **4a** and reagent **1** (standard state: 25 °C, 1 mol/L).

suggests that the incorporation of the dimethyl group leads to a smaller angle of C-C-N in **IM5**, thus facilitating the cyclization process.

For another reaction (Fig. 3), it starts with the electrophilic addition of **IM1** to olefinic double bond in the substrate **4a**, yielding the cyclic iodonium intermediate **IM2'**. Then, the nucleophilic attack of fluoride anion occurs, with an activation energy barrier of 22.7 kcal/mol relative to **IM1**, to give **IM3'**; this process is the rate-limiting step in the reaction. The activation energy barrier of the reaction between **4a** and **AFBI** (22.7 kcal/mol) is lower than that of the reaction between **2a** and **AFBI** (23.5 kcal/mol), which is consistent with the results of the competition experiments (Scheme 4a). To explore the origin of the different chemoselectivity of two reactions, we calculated the energy barriers of the [1,2]-aminoalkyl migration and [1,2]-methyl migration for substrate **4a**. The [1,2]-aminoalkyl migration occurs to give the carbocation intermediate **IM5'** with the release of an Ag(I) complex **G-AgBF$_4$**, which needs to overcome an activation energy barrier of 12.8 kcal/mol relative to **IM4'**. However, the [1,2]-methyl migration has to overcome an activation energy barrier of 16.5 kcal/mol, illustrating that the [1,2]-aminoalkyl migration is more favorable than [1,2]-methyl migration. Finally, **IM5'** forms a six-membered ring product with an intramolecular cyclization, which is exothermic by 61.1 kcal/mol. In conclusion, the expected order of the migration aptitude in **AFBI**-mediated cyclofluorination reactions of *gem*-disubstituted alkenes is aryl > aminoalkyl > methyl.

On the basis of these results and previous reports, we assumed the reaction pathway, in particular, to clarify the reaction sequence: the fluoroiodane(III) reagent **1** is activated by the catalyst AgBF$_4$ to form intermediate **A**, in which the fluorine is coordinated to AgBF$_4$. Then, intermediate **A** undergoes an electrophilic addition to the alkene in *gem*-disubstituted alkenes **2** or **4** to give the cyclic iodonium intermediate **B**. An intramolecular nucleophilic attack of the fluoride occurs at the more-substituted carbon atom because it is better able to stabilize the partial positive charge and form hypervalent iodine(III) intermediate **C** and **D** with the iodoaryl group acting as an excellent leaving group. When R^1 is aryl, the cationic intermediate **F** is produced and imide anion **G** is released. Finally, an intramolecular cyclization occurs, resulting in **3** with fluorination at the quaternary center, along with the release of the *N*-acetyl-2-iodobenzamide **H**. The compound **H** has been isolated and characterized using ^{1}H NMR and ^{13}C NMR. When R^1 is alkyl, the migration rearrangement generated a tertiary carbocation intermediate **E**. Subsequently, tertiary carbocation intermediate **E** undergoes intramolecular nucleophilic attack of the oxygen atom of the amide group to generate product **5**, along with the release of *N*-acetyl-2-iodobenzamide **H** (Fig. 4).

To demonstrate the synthetic utility of this novel method, we used it as the key step in the further conversion of ibuprofen (Scheme 6) [46]. Specifically, we prepared compound **2ac** from ibuprofen, a commercial drug for antipyretic and analgesic, and then we carried out the reaction of **2ac** with **1** and AgBF$_4$ in DCM, which proceeded smoothly to afford **3ac** in 83 % yield.

In summary, we presented a mild Wagner–Meerwein rearrangement fluorination for the synthesis of highly functionalized five/six-membered heterocycles containing a tertiary carbon–fluorine bond. Interestingly, the tunable five/six-membered heterocycles selectivity is achieved by intramolecular Wagner–Meerwein rearrangement fluorination *via* a judicious choice of the group R^1 attached to the C–C double bond. Mechanistic studies including control experiments and isolation of by-product indicated that the reaction follows a fluorination/1,2-aryl or alkyl migration/cyclization cascade reaction, which opens a new pathway of fluorinated heterocycles. The catalyst AgBF$_4$ plays three roles in the reaction: (a) activates the fluoroiodane(III) reagent **AFBI** through an "F-coordination" mode, (b) stabilises the fluoride anion in the fluorination process, and (c) promotes the rearrangement process by coordinating to two oxygen atoms on the benziodazolone skeleton in a *tetra*-coordinated manner. This new system features simple operation, broad substrate scope, high chemoselectivity, and excellent yields. Further development of Wagner–Meerwein rearrangement fluorination reactions using such a strategy and their applications for drug discovery is in progress.

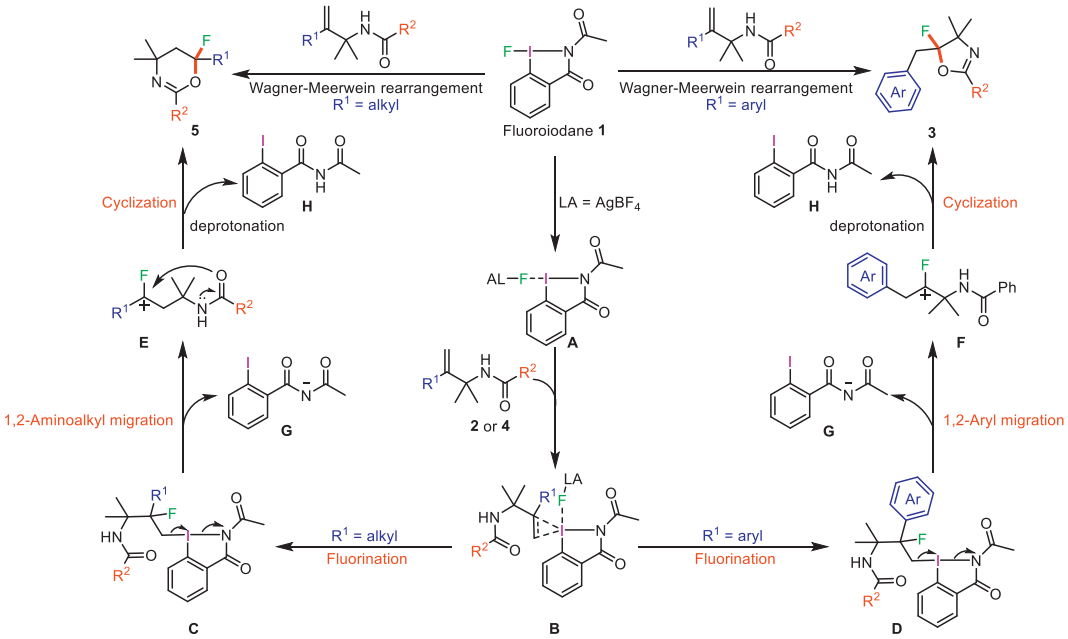
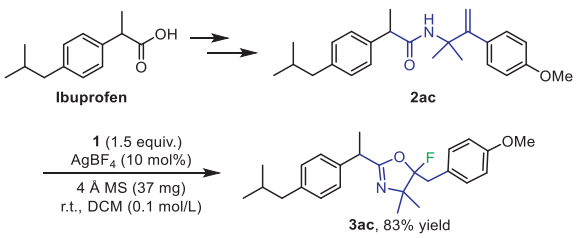


Fig. 4. Proposed mechanism for fluorination–migration–cyclization.



Scheme 6. Further conversion of ibuprofen.

Declaration of competing interest

The authors declare that they have no known competing financial interests or personal relationships that could have appeared to influence the work reported in this paper.

CRediT authorship contribution statement

Jing Ren: Writing – original draft, Investigation. **Feng-Huan Du:** Writing – original draft, Investigation. **Xiaowei Chen:** Investigation. **Chi Zhang:** Writing – review & editing, Project administration, Funding acquisition.

Supplementary materials

Supplementary material associated with this article can be found, in the online version, at doi:10.1016/j.cclet.2025.111407.

References

[1] X.M. Zhang, Y.Q. Tu, F.M. Zhang, Z.H. Chen, S.H. Wang, Chem. Soc. Rev. 46 (2017) 2272–2305.
[2] R.R. Naredla, D.A. Klumpp, Chem. Rev. 113 (2013) 6905–6948.
[3] F.V. Singh, T. Wirth, Synthesis 45 (2013) 2499–2511.
[4] B. Zhang, X. Li, B. Guo, Y. Du, Chem. Commun. 56 (2020) 14119–14136.
[5] S.E. Wengryniuk, S. Canesi, Rearrangements and Fragmentations Mediated by Hypervalent Iodine Reagents, PATAI'S Chemistry of Functional Groups, John Wiley & Sons, Ltd, Chichester, UK, 2018, pp. 665–706.
[6] Z. Yang, Y. Cheng, B. Zhang, et al., Chin. J. Org. Chem. 42 (2022) 3456–3505.
[7] A. Yoshimura, V.V. Zhdankin, Chem. Rev. 124 (2024) 11108–11186.
[8] J. Qurban, M. Elsherbini, T. Wirth, J. Org. Chem. 82 (2017) 11872–11876.
[9] C.B. Pandey, T. Azaz, R.S. Verma, M. Mishra, J.L. Jat, B. Tiwari, J. Org. Chem. 85 (2020) 10175–10181.
[10] J. Zhang, A. Jalil, J. He, et al., Chem. Commun. 57 (2021) 7426–7429.
[11] Q. Wang, M. Biosca, F. Himo, K.J. Szabó, Angew. Chem. Int. Ed. 60 (2021) 26327–26331.
[12] S. Manna, D. Aich, S. Hazra, S. Khandelwal, S. Panda, Chem. Sci. 15 (2024) 4989–4995.
[13] N. Okamoto, Y. Miwa, H. Minami, K. Takeda, R. Yanada, Angew. Chem. Int. Ed. 48 (2009) 9693–9696.
[14] K. Miyamoto, Y. Sakai, S. Goda, M. Ochiai, Chem. Commun. 48 (2012) 982–984.
[15] A. Yoshimura, K.R. Middleton, M.W. Luedtke, C. Zhu, V.V. Zhdankin, J. Org. Chem. 77 (2012) 11399–11404.
[16] R. Oishi, K. Segi, H. Hamamoto, et al., Synlett 29 (2018) 1465–1468.
[17] T. Maegawa, R. Oishi, A. Maekawa, et al., Synthesis 54 (2022) 4095–4103.
[18] X.Q. Li, W.K. Wang, C. Zhang, Adv. Synth. Catal. 351 (2009) 2342–2350.
[19] L.F. Silva, F.A. Siqueira, E.C. Pedrozo, F.Y.M. Vieira, A.C. Doriguetto, Org. Lett. 9 (2007) 1433–1436.
[20] M.S. Yusubov, G.A. Zholobova, I.L. Filimonova, K.W. Chi, Russ. Chem. Bull. Int. Ed. 53 (2004) 1735–1742.
[21] M. Kameyama, F.A. Siqueira, M. Gracia-Mijares, L.F. Silva, M.T.A. Silva, Molecules 16 (2011) 9421–9438.
[22] Y.C. Han, Y.D. Zhang, Q. Jia, J. Cui, C. Zhang, Org. Lett. 19 (2017) 5300–5303.
[23] L.F. Silva, Molecules 11 (2006) 421–434.
[24] L.F. Silva, R.S. Vasconcelos, M.A. Nogueira, Org. Lett. 10 (2008) 1017–1020.
[25] T. Abo, M. Sawaguchi, H. Senboku, S. Hara, Molecules 10 (2005) 183–189.
[26] J. Ren, F.H. Du, M.C. Jia, et al., Angew. Chem. Int. Ed. 60 (2021) 24171–24178.
[27] W.W. Chen, A.B. Cuenca, A. Shafir, Angew. Chem. Int. Ed. 59 (2020) 16294–16309.
[28] J. Tian, F. Luo, Q. Zhang, et al., J. Am. Chem. Soc. 142 (2020) 6884–6890.
[29] W. Carpenter, J. Org. Chem. 31 (1966) 2688–2689.
[30] N.O. Ilchenko, B.O.A. Tasch, K.J. Szabó, Angew. Chem. 126 (2014) 13111–13115.
[31] G.C. Geary, E.G. Hope, A.M. Stuart, Angew. Chem. Int. Ed. 54 (2015) 14911–14914.
[32] A. Andries-Ulmer, C. Brunner, J. Rehbein, T. Gulder, J. Am. Chem. Soc. 140 (2018) 13034–13041.
[33] W.X. Lv, Q. Li, J.L. Li, et al., Angew. Chem. Int. Ed. 57 (2018) 16544–16548.
[34] Z. Zhao, L. Racicot, G.K. Murphy, Angew. Chem. Int. Ed. 56 (2017) 11620–11623.
[35] Z. Zhao, A.J. To, G.K. Murphy, Chem. Commun. 55 (2019) 14821–14824.
[36] E.V. Anslyn, D.A. Dougherty, Modern Physical Organic Chemistry, University Science Books, Sausalito, 2006, p. 658.
[37] K.B. Wiberg, P.R. Rablen, J. Org. Chem. 85 (2020) 11741–11749.
[38] H.A. Sharma, K.M. Mennie, E.E. Kwan, E.N. Jacobsen, J. Am. Chem. Soc. 142 (2020) 16090–16096.
[39] J. Ren, M.C. Jia, F.H. Du, C. Zhang, Chin. Chem. Lett. 33 (2022) 4834–4837.
[40] J. Wu, L. Fu, R. Diao, et al., Green Synth. Catal. 6 (2025) 96–100.
[41] J. Fried, E.F. Sabo, J. Am. Chem. Soc. 76 (1954) 1455–1456.
[42] P.M.A. Calverley, J.A. Anderson, B. Celli, et al., N. Engl. J. Med. 356 (2007) 775–789.
[43] G.M. Keating, A. Vaidya, Drugs 74 (2014) 273–282.
[44] B. Zhou, T. Yan, X.S. Xue, J.P. Cheng, Org. Lett. 18 (2016) 6128–6131.
[45] B. Zhou, X.S. Xue, J.P. Cheng, Tetrahedron Lett. 58 (2017) 1287–1291.
[46] M.W. Ha, S.M. Paek, Molecules 26 (2021) 4792.